Corrosion Science 217 (2023) 111139

Contents lists available at ScienceDirect

Corrosion Science

journal homepage: www.elsevier.com/locate/corsci

On the estimation of standard adsorption free energy from corrosion inhibition efficiencies

Anton Kokalj

Department of Physical and Organic Chemistry, Jožef Stefan Institute, Jamova 39, SI-1000 Ljubljana, Slovenia

ARTICLE INFO

Keywords:
Standard adsorption free energy
Corrosion inhibition
Surface coverage
Adsorption isotherm

ABSTRACT

The standard adsorption Gibbs energy (ΔG°_{ads}) is often estimated by assuming that the corrosion inhibition efficiency is equivalent to fractional surface coverage. However, Lindsay et al. [Corros. Sci. 155 (2019) 182–185] demonstrated that this assumption is not necessarily valid. Therefore, a model that maps inhibition efficiency to fractional surface coverage is developed herein to provide a more reliable estimation of ΔG°_{ads}. The model is validated with the experimental data of Lindsay et al.; the analysis confirms their conclusion that a significant error in ΔG°_{ads} estimation can be made by using inhibition efficiency as a proxy for surface coverage.

1. Introduction

In many corrosion inhibition studies, the standard adsorption Gibbs energies (ΔG°_{ads}) of corrosion inhibitors are often estimated by assuming that the corrosion inhibition efficiency (η) is a reliable proxy for the fractional surface coverage (θ), i.e., $\theta \approx \eta$. An adsorption isotherm is then used (several different isotherms may be tested) to link the fractional surface coverage with the inhibitor concentration in the bulk solution, and in doing so, the adsorption equilibrium constant (K) is obtained from which ΔG°_{ads} is calculated.

In this procedure, the c/θ vs. c plot is usually utilized, where the intercept at $c = 0$ is K^{-1}. For example, on the c/θ plot, the Langmuir adsorption isotherm corresponds to the $c/\theta = K^{-1} + c$ line. Hence, K is straightforwardly estimated with the linear regression as the inverse of the intercept. However, during the linear regression, both the intercept and the slope are fitted, which implies that the actual equation is $c/\theta = K^{-1} + nc$, with n being the slope. But this equation is not equivalent to the Langmuir adsorption isotherm. In the first study of this series [1], a theoretical basis for this equation was established. It was demonstrated to be an effective equation that can decently describe various adsorption models. However, any significant deviation from the slope of 1 signals non-Langmuir adsorption due to inter-adsorbate interactions, multi-site adsorption, or surface heterogeneity. Among these causes, only attractive inter-adsorbate interactions lead to a slope of less than 1.

In the second study of this series [2], a detailed analysis of the c/θ dependence on c led to an improved method for estimating the intercept on the c/θ plot via a newly devised empirical adsorption isotherm. It was shown [2] that this new isotherm could accurately describe many different Type–I adsorption isotherms. This new adsorption isotherm can therefore provide a relatively accurate estimate of the standard adsorption Gibbs energy, provided surface coverages are reliably determined experimentally. However, in corrosion inhibition studies, inhibition efficiency is usually used as a proxy for fractional surface coverage, and Lindsay et al. [3] recently demonstrated experimentally that this assumption is not necessarily valid.

For this reason, we scrutinize herein the consequence of using the $\theta \approx \eta$ assumption[1] and provide a sound model that maps inhibition efficiency to fractional surface coverage, i.e., $\theta = f(\eta)$. With this model, we reanalyze the experimental data of Lindsay et al. [3] and confirm their conclusion that by using the $\theta \approx \eta$ assumption, a significant error in ΔG°_{ads} can be made (for their considered case, the error is about 5 kJ/mol, which corresponds to the relative error of 20%).

2. Results and discussion

A glossary of terms is provided at the end of the article to aid in interpreting various symbols used herein.

E-mail address: tone.kokalj@ijs.si.
URL: http://www.ijs.si/ijsw/K3-en/Kokalj.

[1] This assumption was named as *perfect adsorption hypothesis* in [4] ("perfect" because it presupposes that an inhibitor molecule perfectly blocks the corrosion at the surface site where it is adsorbed).

https://doi.org/10.1016/j.corsci.2023.111139
Received 31 December 2022; Received in revised form 23 March 2023; Accepted 24 March 2023
Available online 29 March 2023

2.1. The functional dependence of coverage on inhibition efficiency

Let us assume that an adsorbed inhibitor molecule does not protect only the site at which it is adsorbed but instead some local region around itself; say, it protects m sites. This assumption suggests the $\eta = m\theta$ relation. However, this relation can only hold at low coverage because when the coverage approaches $\theta \to m^{-1}$, the surface is already fully protected ($\eta \to 1$) and η cannot increase further, which implies $\partial\eta/\partial\theta = 0$ at high coverage. Therefore, the boundary conditions for η are:

$$\begin{aligned} &\text{for } \theta = 0: \quad \eta = 0 \quad \text{and} \quad \frac{\partial\eta}{\partial\theta} = m, \\ &\text{for } \theta = 1: \quad \eta = 1 \quad \text{and} \quad \frac{\partial\eta}{\partial\theta} = 0, \end{aligned} \tag{1}$$

A function that fulfills these boundary conditions is:

$$\eta = 1 - (1-\theta)^m. \tag{2}$$

This equation was derived with the assumption that $m > 1$. However, a case where adsorbed inhibitor molecules do not perfectly protect the covered adsorption sites can also be envisaged. In this case, $m < 1$, and we can consider two possibilities. The simpler one is given by a simple linear relation:

$$\eta = m\theta \qquad (\text{for } m \le 1), \tag{3}$$

which is physically acceptable for $m \le 1$ because, at $\theta = 1$, the inhibition efficiency is $\eta = m \le 1$. The second possibility is given by Eq. (2). This equation behaves well also for $m \le 1$. Its interpretation is that at low coverage, $\eta = m\theta$ (i.e., a standalone adsorbed molecule only partially protects a site at which it is adsorbed), but as the coverage increases, the protection becomes better because neighboring molecules help each other at achieving better protection.

Eq. (2) can be further adjusted by assuming that the maximum achievable inhibition efficiency for a given inhibitor is $\eta_{\max} < 1$, i.e., an inhibitor does not entirely prevent corrosion at the full monolayer coverage. The corresponding equation is:

$$\eta = \eta_{\max}(1 - (1-\theta)^{m/\eta_{\max}}), \qquad \text{where } \eta_{\max} \in [0,1]. \tag{4}$$

The exponent is purposely chosen as $m/\eta_{\max}$ so that the equation gives the $\partial\eta/\partial\theta = m$ at $\theta = 0$. The corresponding relation between the inhibition efficiency and surface coverage is plotted in Fig. 1 for $\eta_{\max} = 0.9$ and $m = 3$ and $1/3$.

Eq. (4) requires two parameters, $\eta_{\max}$ and m. The first parameter can be estimated by measuring inhibition efficiencies at relatively high inhibitor concentrations. To estimate the value of m, a surface coverage needs to be determined for at least one concentration at which the η value was also measured. For the so-obtained θ and η pair, the m parameter is calculated from Eq. (4) as:

$$m = \eta_{\max}\frac{\ln(1-\eta/\eta_{\max})}{\ln(1-\theta)}. \tag{5}$$

But a more reliable estimation of m can be obtained by fitting the θ and η values, measured at several different inhibitor concentrations, by Eq. (4).

2.2. Error analysis

In corrosion inhibition studies, standard adsorption Gibbs energy is usually estimated from the c/θ vs. c plot. However, in doing so, the $\eta \approx \theta$ assumption is used, which implies that $\Delta G^{\circ}_{\text{ads}}$ is actually estimated from the c/η vs. c plot. This approach is justified only when the $\eta \approx \theta$ assumption holds. Otherwise, errors are inevitably introduced. To scrutinize them, a similar approach as used in the preceding study [1] is pursued. Hence, we analyze the above-developed model that associates η with θ for a few different adsorption isotherms. To this end, we need

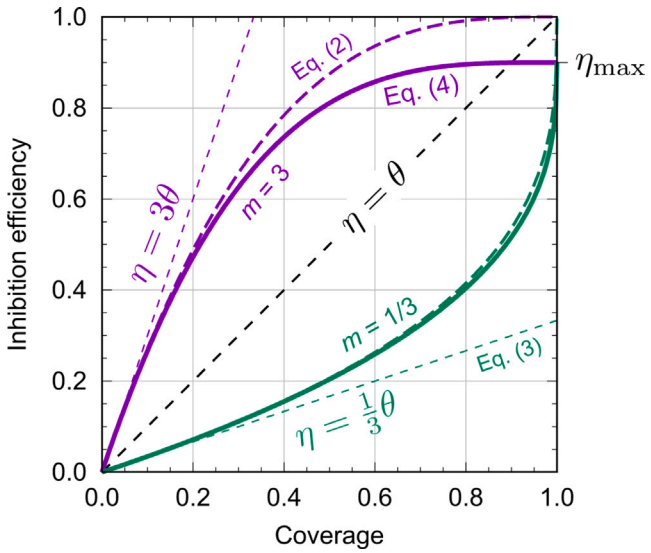

Fig. 1. The relation between the inhibition efficiency and the surface coverage as given by the current model for $m = 1/3$ (green) and $m = 3$ (purple). Solid curves correspond to Eq. (4) with $\eta_{\max} = 0.9$, thick dashed curves to $\eta_{\max} = 1$, and thin dashed lines to Eq. (3). (For interpretation of the references to color in this figure legend, the reader is referred to the web version of this article.)

to invert Eq. (4) and express the coverage as a function of the inhibition efficiency, i.e.:

$$\theta = 1 - \left(1 - \frac{\eta}{\eta_{\max}}\right)^{\eta_{\max}/m}. \tag{6}$$

With this expression for the coverage, let us first see how the Langmuir adsorption isotherm appears on the c/η vs. c plot. For $m < 1$, also the simpler model of Eq. (3) is used, according to which $\theta = m^{-1}\eta$. The adsorption isotherm can be plotted parametrically, where η is used as a parameter. In particular, the $x \equiv c = \theta(\eta)/(K(1-\theta(\eta)))$ and $y \equiv c/\theta = 1/(K(1-\theta(\eta)))$ pairs are plotted for η ranging from 0 to $\eta_{\max}$, where K is the adsorption equilibrium constant. The intercept and the slope at $c = 0$ on the c/η vs. c plot can be derived analytically. To this end, let us approximate the Langmuir adsorption isotherm with the Taylor series up to the second order in η, i.e.:

$$Kc = \frac{\theta}{1-\theta} = \frac{1-\left(1-\frac{\eta}{\eta_{\max}}\right)^{\eta_{\max}/m}}{\left(1-\frac{\eta}{\eta_{\max}}\right)^{\eta_{\max}/m}} \approx \frac{1}{m}\eta + \frac{m+\eta_{\max}}{2m^2\eta_{\max}}\eta^2. \tag{7}$$

This expression can be rearranged to:

$$\frac{c}{\eta} \approx \frac{1}{K}\left[\frac{1}{m} + \frac{m+\eta_{\max}}{2m^2\eta_{\max}}\eta\right]. \tag{8}$$

It is worth noting that the first-order expansion gives a useful expression for η at a very low concentration, i.e., $\eta = mKc$. Hence, by plugging this expression for η into the above equation, we get:

$$\begin{aligned} &\frac{c}{\eta} \approx \frac{1}{mK} + \frac{m+\eta_{\max}}{2m\eta_{\max}}c, \quad \text{hence} \\ &\text{at } c = 0: \quad \text{intercept} = \frac{1}{mK}, \quad \text{slope} = \frac{m+\eta_{\max}}{2m\eta_{\max}}. \end{aligned} \tag{9}$$

Note that for $m = 1$ and $\eta_{\max} = 1$, the $\theta = \eta$ relation holds, and the equation transforms to the Langmuir adsorption isotherm:

$$\frac{c}{\theta} = \frac{1}{K} + c, \quad \text{which is equivalent to} \quad Kc = \frac{\theta}{1-\theta}. \tag{10}$$

At very high concentrations, c/η eventually becomes proportional to c with the slope of $\eta_{\max}^{-1}$ and this relation holds for Type–I isotherms

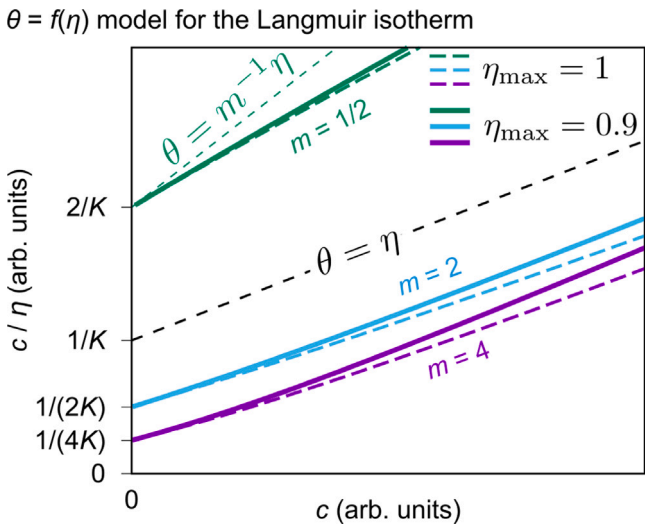

Fig. 2. The Langmuir adsorption isotherm on the c/η vs. c plot with the surface coverage linked to inhibition efficiency via Eq. (6) for $m = 1/2$, 2, and 4. Solid curves correspond to $\eta_{max} = 0.9$ and thick dashed curves to $\eta_{max} = 1$.

for which the saturation coverage is normalized to 1, i.e.:

$$\frac{c}{\eta} = \text{intercept} + \eta_{max}^{-1} c \quad \text{(for Type–I isotherms at high } c\text{)}. \tag{11}$$

The reason is that coverage increases with increasing concentration until eventually a full monolayer coverage is reached,[2] $\theta \approx 1$. From this point on, $c/\theta \approx c/1 = c$. But $\theta = 1$ corresponds to $\eta = \eta_{max}$. Hence, c/η becomes proportional to c/η_{max}, which implies the slope of η_{max}^{-1}.

Within the current model, the Langmuir adsorption isotherm on the c/η vs. c plot is a curve whose details depend on the m and η_{max} parameters of Eq. (6). Fig. 2 shows several exemplar Langmuir curves for $m = 0.5$, 2, 4, and $\eta_{max} = 0.9$ and 1. According to Eqs. (9) and (11), the slope of the Langmuir isotherm on the c/η vs. c plot changes from $(m + \eta_{max})/(2m\eta_{max})$ at $c = 0$ to η_{max}^{-1} at very high c, yet Fig. 2 reveals that these curves are sufficiently linear that can be fitted by the linear equation:

$$\frac{c}{\eta} = \frac{1}{K_{fit}} + nc. \tag{12}$$

It was demonstrated in the previous publication [1] that the analogous $c/\theta = 1/K_{fit} + nc$ equation could fit quite well various adsorption isotherms. Here, we use c/η instead of c/θ to align with the usual procedure where η is used as an estimate for θ. The problem in doing so is that the intercept on the c/θ plot, which is actually the c/η plot, is interpreted as the inverse of the adsorption equilibrium constant, whereas Eq. (9) reveals that the intercept is $1/(mK)$. For m sufficiently different from 1, the error is thus considerable. For example, for $m = 4$, the estimated K_{fit} is four times greater than the actual K. Luckily, due to the logarithmic dependence of ΔG°_{ads} on K (i.e., $\Delta G^{\circ}_{ads} \propto -RT \ln Kc^{\circ}$, where c° is the standard concentration of 1 M), a large error in K results in a considerably smaller error in ΔG°_{ads}. To foresee that this is so, note that for $K_{fit} = mK$, the relation between the so-estimated standard adsorption Gibbs energy (ΔG^{fit}_{ads}) and the true ΔG°_{ads} is:

$$\Delta G^{fit}_{ads} = \Delta G^{\circ}_{ads} - RT \ln m. \tag{13}$$

At room temperature, the $RT \ln m$ term is 1.7, 2.7, 3.4, and 4.0 kJ/mol for $m = 2$, 3, 4, and 5, respectively. These error estimates are based on Eq. (9), which holds only for $c \to 0$. But at finite concentrations, a further error is introduced when adsorption isotherm on the c/η vs. c plot is curvy and is fitted by linear Eq. (12). An example of a considerably nonlinear isotherm on the c/η vs. c plot are attractive Frumkin isotherms (Fig. 3a). In contrast, repulsive Frumkin isotherms are much less curvy (Fig. 3b). The Frumkin isotherm can be written as:

$$Kc = \frac{\theta}{1-\theta} \exp(2w\theta), \tag{14}$$

where w is the parameter that describes lateral interactions between adsorbed molecules ($w < 0$ for attraction and $w > 0$ for repulsive interactions).

To estimate this nonlinear error, a series of "virtual" experiments were performed, where the currently developed model that links inhibition efficiency and coverage was utilized. To this end, room temperature and ΔG°_{ads} of −30 kJ/mol were assumed[3] and data points were generated in the concentration range from 0.01 to 2 mM with the Langmuir and Frumkin adsorption isotherms for several different values of m in the $m \in [0.2, 6]$ range and $\eta_{max} = 1$. The so-generated data points were fitted with Eq. (12), and the resulting standard adsorption Gibbs energies (ΔG^{fit}_{ads}) were compared to the actual ones, i.e., the error was evaluated as the $\Delta G^{fit}_{ads} - \Delta G^{\circ}_{ads}$ difference. The dependence of this difference on the parameter m is shown in Fig. 4a. The figure reveals that Eq. (13) provides a correct error trend and thus a good first-order estimate. Note that the errors for the Langmuir adsorption isotherms are between those for repulsive and attractive Frumkin adsorption isotherms. The latter isotherm is the most nonlinear, and its nonlinear errors (i.e., the difference between the actual error and the $-RT \ln m$ estimate) are the most significant (Fig. 4b). In the shown m range, the nonlinear errors for the repulsive Frumkin isotherm are within about ±0.7 kJ/mol. For the Langmuir isotherm, the nonlinear error magnitudes reach about 1.5 kJ/mol and, for the attractive Frumkin isotherm, about 2.5 kJ/mol at the highest considered m value.

2.3. Reinterpreting the Villamil equation

The slope n in the $c/\theta = K^{-1} + nc$ equation is occasionally interpreted as the number of sites the inhibitor molecule adsorbs to. In this context, the Villamil equation [6] is often utilized:

$$\frac{c}{\theta} = \frac{n}{K} + nc. \tag{15}$$

However, Villamil et al. did not explain how this equation emerges. It was shown in the previous study [1] that in the case of multi-site adsorption, the $c/\theta = K^{-1} + nc$ equation should be preferable to the Villamil Eq. (15).

The currently developed model that maps inhibition efficiency to surface coverage allows for a different interpretation of the Villamil equation. In particular, for $m < 1$, the simpler model of Eq. (3) gives $\theta = m^{-1}\eta$. By plugging this expression into the Langmuir adsorption isotherm, we obtain:

$$\frac{c}{\theta} = \frac{c}{m^{-1}\eta} = \frac{1}{K} + c, \tag{16}$$

hence:

$$\frac{c}{\eta} = \frac{m^{-1}}{K} + m^{-1}c. \tag{17}$$

It should be noted that when the $\theta = \eta$ assumption is used, one actually considers c/η instead of c/θ. By taking this into account, the comparison between Eq. (17) and Eq. (15) reveals that $n = m^{-1}$. This suggests that within the Langmuir adsorption model, n in the Villamil

[2] For a given solute, a monolayer coverage may require concentration beyond the saturation concentration. In such a case, a hypothetical auxiliary solute that is equivalent to the real solute but displays an unlimited solubility can be envisaged.

[3] This value is compatible with many reported ΔG°_{ads} values in the corrosion inhibition literature. It is in between the threshold values of −20 and −40 kJ/mol that are usually used to distinguish between physisorption and chemisorption. This 20/40 rule was criticized recently [5] by arguing that it is not a reliable criterion to distinguish between the two adsorption modes.

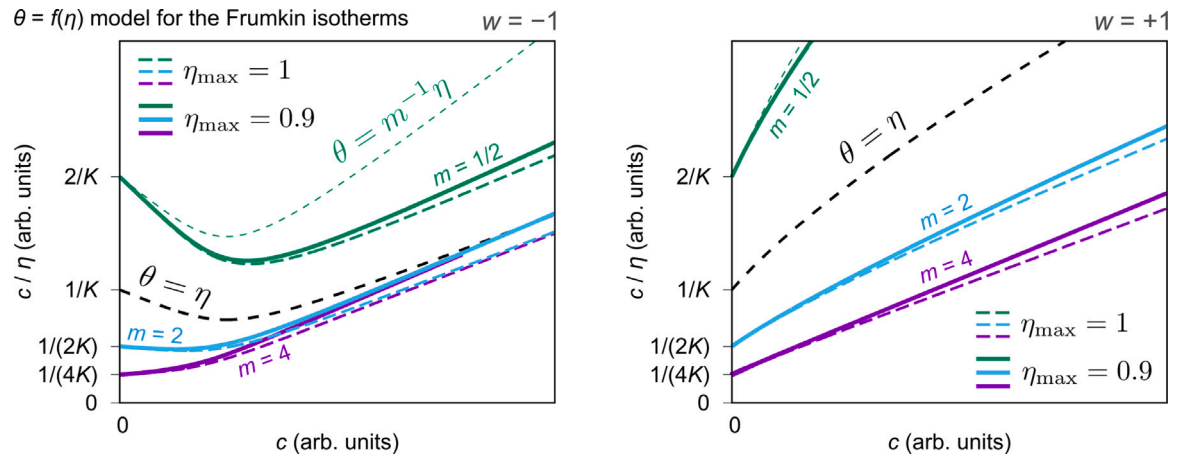

Fig. 3. The attractive (left, $w = -1$) and repulsive (repulsive, $w = +1$) Frumkin isotherms on the c/η vs. c plot with the coverage transformed to inhibition efficiency via Eq. (6) for $m = 1/2$, 2, and 4. Solid curves correspond to $\eta_{max} = 0.9$, thick dashed curves to $\eta_{max} = 1$, and black dashed curve to $\theta = \eta$. A thin dashed curve corresponds to a simpler model of $\theta = m^{-1}\eta$.

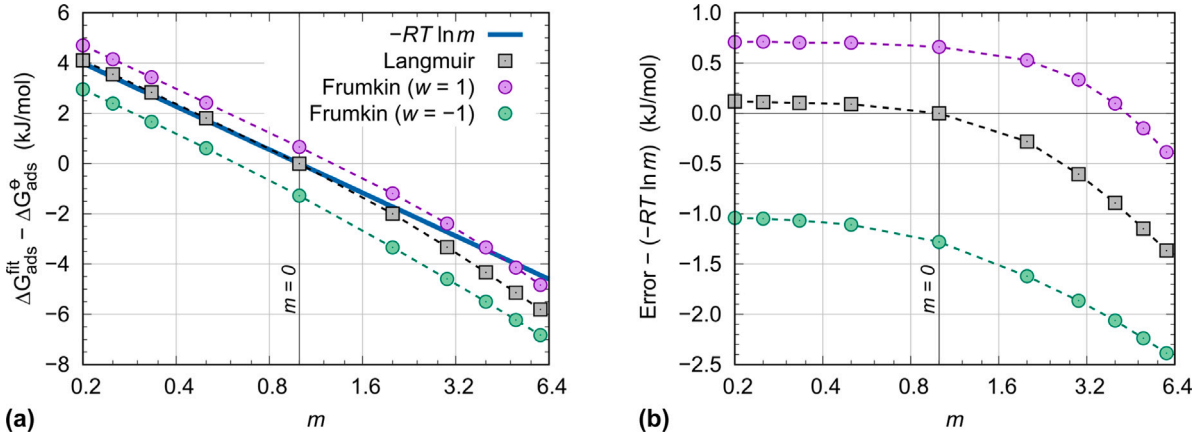

Fig. 4. Error analysis performed for the Langmuir, attractive Frumkin, and repulsive Frumkin adsorption isotherms using "virtual" experiments (see text) and the current model that associates inhibition efficiency with the surface coverage. (a) Dependence of the $\Delta G^{fit}_{ads} - \Delta G^{\ominus}_{ads}$ difference on the parameter m, where ΔG^{fit}_{ads} is the estimated standard adsorption Gibbs energy with Eq. (12) using the $\theta = \eta$ assumption and $\Delta G^{\ominus}_{ads}$ is the true standard adsorption Gibbs energy. (b) The difference between the whole error ($\Delta G^{fit}_{ads} - \Delta G^{\ominus}_{ads}$) and its first-order approximation ($-RT \ln m$).

equation is not related to the number of sites the molecule adsorbs to but rather to the inverse of the "protection efficiency" m, but only for $m < 1$ cases (for $m > 1$, m is the number of protected sites by a single inhibitor molecule at low coverage, but for $m < 1$, an inhibitor molecule incompletely protects the site at which it is adsorbed with the efficiency m).

2.4. Evaluating the current model with experimental data

Lindsay et al. [3] evaluated the performance of 2-merceptobenzimidazole as a corrosion inhibitor for carbon steel in 1 M HCl and, in addition, to determining the inhibition efficiency at nine different inhibitor concentrations, also performed an XPS-based analysis of adsorbed inhibitor layers and estimated the inhibitor coverage at four different inhibitor concentrations. Although surface coverages are not determined directly with XPS but are instead usually derived from XPS-peak intensities using some model,[4] we tacitly assume they are more reliable than the IE-derived coverages and can be taken as a reference. If, instead, the XPS-derived coverages are subject to significant systematic errors, the m parameter in Eq. (4) can be seen as an effective parameter that makes the XPS- and IE-derived coverages compatible with each other. In this case, the estimated m value is susceptible to a systematic error. The effect of this error on the value of the standard adsorption Gibbs energy can be evaluated with the error analysis of Section 2.2 (cf. Fig. 4).

Based on their study, we can thus test the current model of Eq. (6) that links the inhibition efficiency with the surface coverage. These authors estimated the standard adsorption Gibbs energy by fitting both the inhibition efficiencies (IE) and XPS-deduced coverages with the Langmuir adsorption isotherm and reported the difference of 5.5 kJ/mol between the IE- and XPS-deduced $\Delta G^{\ominus}_{ads}$ values. They also argued that the Langmuir adsorption isotherm might not provide a very accurate estimate of $\Delta G^{\ominus}_{ads}$ due to the relatively poor fit quality. It is well accepted that 2-merceptobenzimidazole can adsorb in two different forms (thiolate and thione) [9–13], and for this reason, authors also used an expression involving the sum of two independent

[4] In particular, Lindsay et al. estimated the surface coverage by fitting the XPS-peak intensities ratios at two photoelectron emission angles, assuming that the surface region consists of a topmost layer of adventitious carbon, a 2D monolayer of 2-merceptobenzimidazole, and the carbon-steel substrate [7]. The authors mentioned that there are likely to be systematic errors associated with surface coverage determinations. Still, they assumed that these errors are not too significant [8].

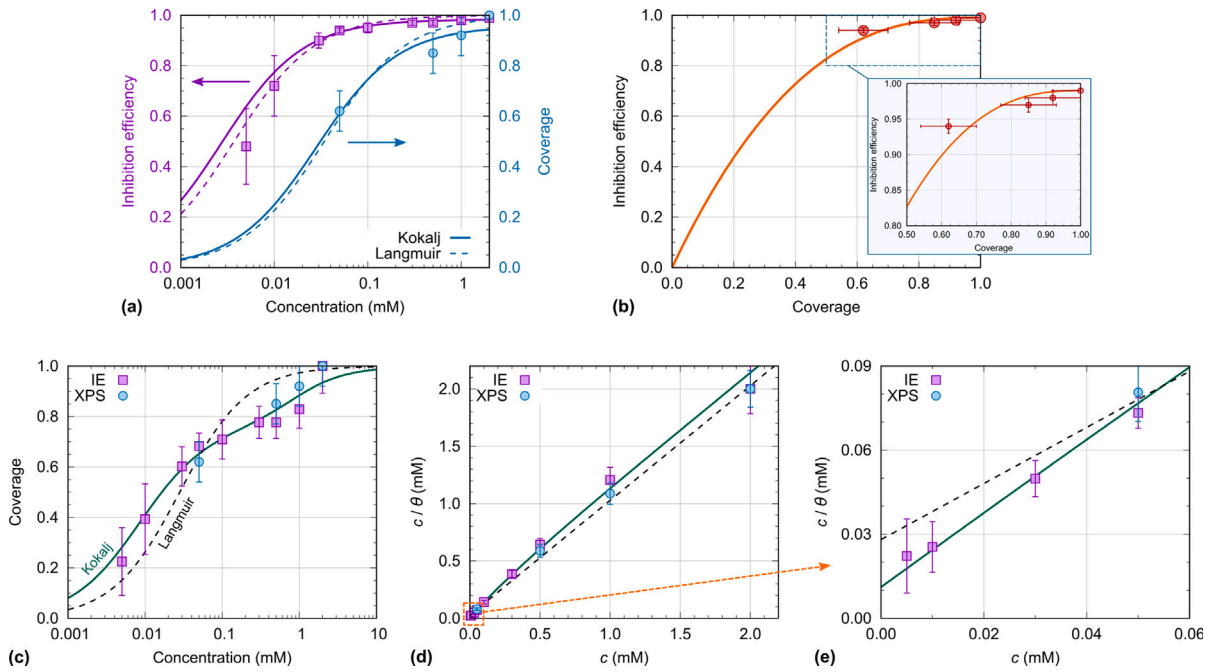

Fig. 5. (a) Experimental inhibition efficiencies and XPS-derived coverages of Lindsay et al. [3] fitted with the Langmuir (dashed curves) and Kokalj (solid curves) isotherms. (b) The relation between the inhibition efficiency and surface coverage as predicted with the current model by fitting the experimental data. (c) XPS- and IE-derived coverages vs. concentrations fitted with the Langmuir and Kokalj adsorption isotherms. (d and e) The c/θ vs. c plots of the merged XPS- and IE-derived data; (d) shows the whole concentration range and (e) is a zoom-in to lower concentrations; particularly (e) suggests that Kokalj isotherm better fits the data and, consequently, provides a more reliable estimate of the standard adsorption Gibbs energy.

adsorption isotherms. To cope with this issue, a new empirical general-purpose isotherm introduced in the previous study [2] is used here (named the Kokalj isotherm). The expression for this isotherm is [2]:

$$\theta = \frac{c}{\frac{1}{K} + nc + c_1\left[\exp\left(-\frac{c}{c_2}\right) - 1\right]}, \tag{18}$$

where c is the molar concentration, K is the adsorption equilibrium constant (in M^{-1} units), and n, c_1, and c_2 are empirical (fitting) parameters. Note that n is unitless (its value is typically close to 1), while c_1 and c_2 have a unit of concentration; c_1 can be positive or negative, but c_2 is constrained to be positive.

The data of Lindsay et al. [3] are shown in Fig. 5a. Both the IE values and XPS-derived coverages are fitted with the Langmuir and Kokalj isotherms. The IE values fitted with the Langmuir isotherm give $\Delta G^{\circ}_{ads} = -31.0 \pm 0.4$ kJ/mol, whereas XPS-derived coverages give $\Delta G^{\circ}_{ads} = -25.5 \pm 0.6$ kJ/mol; these values are in excellent agreement with the ΔG°_{ads} values of Lindsay et al.[5] In contrast, Kokalj isotherm gives $\Delta G^{\circ}_{ads} = -31.8 \pm 0.4$ kJ/mol and $\Delta G^{\circ}_{ads} = -25.9 \pm 1.1$ kJ/mol for the IE- and XPS-derived coverages, respectively. For the estimations based on the Kokalj isotherm, the value of the n parameter was fixed to 1 because good physical reason exists that $n \approx 1$ when high coverages are considered [2], which is currently the case (cf. Fig. 5a).

Fig. 5b shows the relationship between the inhibition efficiency and the XPS-derived coverage. The current model of Eq. (4) fits the four experimental data points rather decently; the resulting values are $m = 2.58$ and $\eta_{max} = 0.99$. Once the relation between the inhibition efficiency and coverage was established, the IE values were converted to coverage (named as IE-derived coverages in the following) and used to provide a better estimate of ΔG°_{ads}. Fig. 5c shows the XPS- and IE-derived coverages as a function of the inhibitor concentration; the green solid curve shows the fit of the data points with the Kokalj isotherm, whereas the black dashed curve shows the fitted Langmuir isotherm. It is evident that the Kokalj isotherm better fits the experimental data points than the Langmuir isotherm. Further confirmation of this observation is provided by the c/θ vs. c plot of Fig. 5d and its low concentration zoom-in, shown in Fig. 5e. The ΔG°_{ads} value obtained with the Kokalj isotherm is -27.1 ± 0.5 kJ, whereas the Langmuir isotherm gives the value of -26.0 ± 0.5 kJ/mol; for the description of the error estimation, see Appendix B. Not surprisingly, these two ΔG°_{ads} values are much closer to the original ΔG°_{ads} value, derived from XPS-deduced coverage, than to the IE-derived ΔG°_{ads} value. However, the current values are based on more data points than the original XPS-derived value and should therefore be more reliable. This suggests that, currently, the best estimate of ΔG°_{ads} is provided by the Kokalj isotherm on XPS- and IE-derived coverages, being -27.1 ± 0.5 kJ. Whether this inference is correct can be established experimentally by new XPS or any other suitable measurements to estimate coverages for a larger set of different inhibitor concentrations.

The new analysis reconfirms the conclusion of Lindsay et al. [3] that, in this particular case, the error made by using $\eta \approx \theta$ approximation in estimating ΔG°_{ads} is about 5 kJ/mol. This error is in the range predicted by the error analysis of Fig. 4a.

[5] It is usually assumed that corrosion inhibitor molecules substitute adsorbed water molecules during adsorption, $Mol_{(sol)} + H_2O_{(ads)} \rightleftharpoons Mol_{(ads)} + H_2O_{(sol)}$. Consequently, the relation between the adsorption equilibrium constant and the standard adsorption Gibbs energy is given by:

$$K = \frac{1}{c_{H_2O}} \exp\left(-\frac{\Delta G^{\circ}_{ads}}{RT}\right), \tag{19}$$

where c_{H_2O} is the molar concentration of water solvent. However, Lindsay et al. [3] assumed a plain adsorption, $Mol_{(sol)} \rightleftharpoons Mol_{(ads)}$. Hence, the corresponding relation is:

$$K = \frac{1}{c^{\circ}} \exp\left(-\frac{\Delta G^{\circ}_{ads}}{RT}\right), \tag{20}$$

where c° is the standard state inhibitor concentration of 1 M. At room temperature, the ΔG°_{ads} values obtained from the two equations differ by 10 kJ/mol [1]. To be in line with the study of Lindsay et al. also herein the ΔG°_{ads} values are calculated by the latter equation.

3. Conclusions

A simple model associating the inhibition efficiency with the fractional surface coverage was presented. Alongside, the consequence of using the $\theta \approx \eta$ assumption was scrutinized. The model was validated with the experimental data of Lindsay et al. [3], and the analysis performed with the new model confirms their conclusion. For cases where θ and η differ, a considerable error can be made in estimating the adsorption equilibrium constant K. Luckily, due to the logarithmic dependence of standard adsorption Gibbs energy $\Delta G^{\circ}_{\mathrm{ads}}$ on K, a considerable error in K results in a much smaller error in $\Delta G^{\circ}_{\mathrm{ads}}$. Nevertheless, the $\Delta G^{\circ}_{\mathrm{ads}}$ error may still be significant.

The presented model depends on two parameters: m (the number of adsorption sites protected by a single inhibitor molecule at low coverage) and $\eta_{\max}$ (the maximum inhibition efficiency of a given inhibitor). The model requires the knowledge of the experimentally determined $\eta_{\max}$ value and reliable estimation of surface coverage for at least one concentration at which the η value was measured (but the model becomes more reliable if both θ and η are estimated for several concentrations).

Glossary

IE – inhibition efficiency

XPS – X-ray photoelectron spectroscopy

$\Delta G^{\circ}_{\mathrm{ads}}$ – standard adsorption Gibbs energy

$\Delta G^{\mathrm{fit}}_{\mathrm{ads}}$ – the value of $\Delta G^{\circ}_{\mathrm{ads}}$ obtained by fitting the experimental data

K – adsorption equilibrium constant

K_{fit} – the value of K obtained by fitting the experimental data

θ – fractional surface coverage ranging from 0 to 1

η – inhibition efficiency ranging from 0 to 1 (for inhibitors)

$\eta_{\max}$ – maximum achievable inhibition efficiency of a given inhibitor

m – the number of surface sites protected by a single adsorbed inhibitor molecule at low coverage; it is the main parameter of the current model that links η with θ

n – the slope of the regression line on the c/θ vs. c plot and the unitless parameter of the Kokalj isotherm

c_1, c_2 – the other two parameters of the Kokalj isotherm, expressed in the units of concentration

$c_{\mathrm{H_2O}}$ – molar concentration of liquid water

c° – standard concentration of 1 M

w – parameter describing lateral interactions in the Frumkin adsorption isotherm

R – gas constant

T – temperature

CRediT authorship contribution statement

Anton Kokalj: Conceptualization, Methodology, Investigation, Formal analysis, Writing – original draft, Writing – review & editing, Visualization.

Declaration of competing interest

The author declares that he has no known competing financial interests or personal relationships that could have appeared to influence the work reported in this paper.

Data availability

The data used by the manuscript are contained within it, whereas the scripts used for fitting and generating the graphs will be made available on request.

Acknowledgments

This work has been financially supported by the Slovenian Research Agency (Grant No. P2-0393).

Appendix A. Technical details

Graphs were plotted with the Gnuplot software [14], and their post-processing was done in Inkscape [15]. Gnuplot was also used for fitting. Derivation of equations was facilitated with WolframAlpha [16].

Appendix B. Error estimation

Errors were estimated using total differential and absolute values of the component errors, i.e.:

$$\Delta f(x,y,z) = \left|\frac{\partial f}{\partial x}\Delta x\right| + \left|\frac{\partial f}{\partial y}\Delta y\right| + \left|\frac{\partial f}{\partial z}\Delta z\right|, \tag{B.1}$$

where Δx, Δy, and Δz are the estimated errors of the parameters x, y, and z.

For the XPS-derived coverages, the experimental error estimates provided in [3] were used. In contrast, the IE-derived coverages were estimated from the experimental IE values [3] via Eq. (6), and their error estimates were calculated as:

$$\begin{aligned}\Delta\theta = {} & \frac{\left(1-\frac{\eta}{\eta_{\max}}\right)^{(\eta_{\max}/m)-1}}{m}\Delta\eta \\ & + \left|\frac{\eta_{\max}\left(1-\frac{\eta}{\eta_{\max}}\right)^{\eta_{\max}/m}\ln\left(1-\frac{\eta}{\eta_{\max}}\right)}{m^2}\right|\Delta m \\ & + \left|\frac{\left(1-\frac{\eta}{\eta_{\max}}\right)^{\eta_{\max}/m}\left[\eta+(\eta_{\max}-\eta)\ln\left(1-\frac{\eta}{\eta_{\max}}\right)\right]}{m(\eta_{\max}-\eta)}\right|\Delta\eta_{\max},\end{aligned} \tag{B.2}$$

where $\Delta\eta$ is the experimental error estimate for a given inhibition efficiency [3], whereas Δm and $\Delta\eta_{\max}$ are the error estimates of the m and $\eta_{\max}$ parameters as obtained by fitting the IE and coverage data (Fig. 5b). There is a subtlety, though. Eq. (B.2) presupposes that $\eta_{\max}$ is higher than any experimental η value, otherwise the logarithmic terms are not real. Hence, for $\eta_{\max}$, a value of 1.0 was used in Eq. (B.2), which is higher than any experimental η value.

The so-obtained $\Delta\theta$ error estimates were used for fitting the (c,θ) data with the Langmuir and Kokalj isotherms, using the nonlinear least-squares Marquardt–Levenberg algorithm [17,18] as implemented in Gnuplot [14]. The $\Delta\theta$ error estimates were used as weights for data points (a data point with a smaller (larger) $\Delta\theta$ error has a higher (lower) weight). The fit returned the adsorption equilibrium constant K and its error estimate ΔK, form which the standard adsorption Gibbs energy ($\Delta G^{\circ}_{\mathrm{ads}}$) was calculated by Eq. (20), while its error ($\Delta(\Delta G^{\circ}_{\mathrm{ads}})$) was estimated as:

$$\Delta(\Delta G^{\circ}_{\mathrm{ads}}) = RT\frac{\Delta K}{K}. \tag{B.3}$$

References

[1] A. Kokalj, On the use of the Langmuir and other adsorption isotherms in corrosion inhibition, Corros. Sci. 217 (2023) 111112, http://dx.doi.org/10.1016/j.corsci.2023.111112.

[2] A. Kokalj, A new empirical general-purpose adsorption isotherm for improved estimation of standard adsorption free energy, Corros. Sci. (2023) http://dx.doi.org/10.1016/j.corsci.2023.111124, in press.

[3] M.S. Walczak, P. Morales-Gil, R. Lindsay, Determining Gibbs energies of adsorption from corrosion inhibition efficiencies: Is it a reliable approach? Corros. Sci. 155 (2019) 182–185, http://dx.doi.org/10.1016/j.corsci.2019.04.040.

[4] A. Kokalj, Considering the concept of synergism in corrosion inhibition, Corros. Sci. 212 (2023) 110922, http://dx.doi.org/10.1016/j.corsci.2022.110922.

[5] A. Kokalj, Corrosion inhibitors: physisorbed or chemisorbed? Corros. Sci. 196 (2022) 109939, http://dx.doi.org/10.1016/j.corsci.2021.109939.

[6] R.F.V. Villamil, P. Corio, J.C. Rubim, S.M.L. Agostinho, Sodium dodecylsulfate–benzotriazole synergistic effect as an inhibitor of processes on copper|chloridric acid interfaces, J. Electroanal. Chem. 535 (1) (2002) 75–83, http://dx.doi.org/10.1016/S0022-0728(02)01153-1.

[7] P. Morales-Gil, M.S. Walczak, R.A. Cottis, J.M. Romero, R. Lindsay, Corrosion inhibitor binding in an acidic medium: Interaction of 2-mercaptobenizmidazole with carbon-steel in hydrochloric acid, Corros. Sci. 85 (2014) 109–114, http://dx.doi.org/10.1016/j.corsci.2014.04.003.

[8] P. Morales-Gil, M.S. Walczak, C.R. Camargo, R.A. Cottis, J.M. Romero, R. Lindsay, Corrosion inhibition of carbon-steel with 2-mercaptobenzimidazole in hydrochloric acid, Corros. Sci. 101 (2015) 47–55, http://dx.doi.org/10.1016/j.corsci.2015.08.032.

[9] I. Milošev, N. Kovačević, A. Kokalj, Effect of mercapto and methyl groups on the efficiency of imidazole and benzimidazole-based inhibitors of iron corrosion, Acta Chim. Slov. 63 (3) (2016) 544–559, http://dx.doi.org/10.17344/acsi.2016.2326.

[10] N. Kovačević, I. Milošev, A. Kokalj, The roles of mercapto, benzene, and methyl groups in the corrosion inhibition of imidazoles on copper: II. Inhibitor–copper bonding, Corros. Sci. 98 (2015) 457–470, http://dx.doi.org/10.1016/j.corsci.2015.05.041.

[11] D.K. Kozlica, A. Kokalj, I. Milošev, Synergistic effect of 2-mercaptobenzimidazole and octylphosphonic acid as corrosion inhibitors for copper and aluminium – an electrochemical, XPS, FTIR and DFT study, Corros. Sci. 182 (2021) 109082, http://dx.doi.org/10.1016/j.corsci.2020.109082.

[12] E. Vernack, D. Costa, P. Tingaut, P. Marcus, DFT studies of 2-mercaptobenzothiazole and 2-mercaptobenzimidazole as corrosion inhibitors for copper, Corros. Sci. 174 (2020) 108840, http://dx.doi.org/10.1016/j.corsci.2020.108840.

[13] S. Neupane, P. Losada-Pérez, U. Tiringer, P. Taheri, D. Desta, C. Xie, D. Crespo, A. Mol, I. Milošev, A. Kokalj, F.U. Renner, Study of mercaptobenzimidazoles as inhibitors for copper corrosion: Down to the molecular scale, J. Electrochem. Soc. 168 (5) (2021) 051504, http://dx.doi.org/10.1149/1945-7111/abf9c3.

[14] T. Williams, C. Kelley, et al., Gnuplot 5.4, 2020, http://www.gnuplot.info/.

[15] Inkscape Project, Inkscape, 2021, URL https://inkscape.org, version 1.0.2.

[16] Wolfram Research, Inc., Wolfram|Alpha: Computational Intelligence, 2022, URL https://www.wolframalpha.com, (Online; last accessed 23 December 2022).

[17] K. Levenberg, A method for the solution of certain non-linear problems in least squares, Q. Appl. Math. 2 (2) (1944) 164–168, http://dx.doi.org/10.1090/qam/10666.

[18] D.W. Marquardt, An algorithm for least-squares estimation of nonlinear parameters, J. Soc. Ind. Appl. Math. 11 (2) (1963) 431–441, http://dx.doi.org/10.1137/0111030.